Available online at www.sciencedirect.com
ScienceDirect
Trans. Nonferrous Met. Soc. China 23(2013) 53−58
Transactions of Nonferrous Metals Society of China
www.tnmsc.cn

Role of particle stimulated nucleation in recrystallization of hot extruded Al 6061/SiC$_p$ composites

C. S. RAMESH[1,2], R. KESHAVAMURTHY[3], Praveennath G. KOPPAD[1], K. T. KASHYAP[1]

1. Department of Mechanical Engineering, PES Institute of Technology, Bangalore 560085, India;
2. Visiting Professor, School of Design, Engineering and Computing, Bournemouth University, United Kingdom;
3. Central Manufacturing Technology Institute, Tumkur Road, Bangalore 560022, India

Received 12 March 2012; accepted 27 August 2012

Abstract: Studies on texture and microstructure evolution in hot extruded Al 6061 aluminium alloy reinforced with uncoated and nickel coated SiC$_p$ were carried out by electron backscattered diffraction technique. Textures of both the alloy and its composite with nickel coated SiC$_p$ do exhibit strong β fiber with its axis parallel to the direction of extrusion. In addition to the dominant cube texture (001)⟨100⟩, fully recrystallized grains with partially equiaxed structure have been observed in the alloy reinforced with uncoated SiC$_p$. The recrystallization texture of this composite can be attributed to the particle stimulated nucleation (PSN) due to the presence of SiC$_p$ with size less than 5 µm. Under these conditions, the low value of Zener–Hollomon, Z (~ 10^{12} s^{-1}) confirms that PSN is one of the dominant mechanisms for recrystallization and is governed by formation of deformation zone rather than stored energy.

Key words: metal matrix composites; 6061/SiC$_p$ composite; extrusion; particle stimulated nucleation; recrystallization; stored energy

1 Introduction

Aluminium alloys of 6xxx series have been the material of choice for both aerospace and automotive applications because of their attractive properties. These aluminium alloys reinforced with hard and non-deformable ceramic particles such as SiC are of significant importance as they offer better mechanical and tribological properties [1,2]. SiC reinforced aluminium alloy composites can be readily shaped by secondary metal working processes, such as rolling and extrusion. These processes lead to the evolution of new microstructure and texture in aluminium alloys and their composites, which have been reported by few researchers [3,4]. However, the reports on texture evolution in hot extruded aluminium alloy based composites are very limited although the rolling textures of aluminium based composites have been studied in detail. The typical rolling textures of aluminium alloys and its composites are generalized as α and β fibers. The α fiber consists of goss (110)⟨001⟩ and brass (110)⟨112⟩ texture components, while the β fiber ranges from brass (110)⟨112⟩ through the S (123)⟨634⟩ and ends at Cu (112)⟨111⟩.

The deformation and recrystallization behaviour of hot deformed aluminium alloys and composites is still a matter of intense research. POUDENS and BACROIX [3,5] have reported the deformation textures in Al−SiC composites of two fibers ⟨111⟩ and ⟨100⟩. They have observed increase in the intensity of ⟨111⟩ fiber during annealing of particle-free material. In the composites, the intensity of ⟨111⟩ fiber was sharper than the pure alloy when the matrix was reinforced with less than 10% SiC whereas for greater than 10% SiC, a decrease in intensity of ⟨111⟩ fiber was observed. It has been reported that SiC particles favour the particle stimulated nucleation (PSN) by nucleation of new grains in the deformation zones but to a small extent at low extrusion temperatures [6,7]. The recrystallized microstructure depends on the formation of the nuclei and growth in the deformed matrix, but the evolution of recrystallization texture is still a matter of controversy with two competing mechanisms, namely oriented nucleation and oriented growth, trying to describe the origin of recrystallization textures.

The working temperature and the strain rate are related by Zener−Hollomon factor (Z). The factor Z is closely related to the microstructure and texture of the particle containing alloy as it is important to represent the effect of PSN as a function of working temperature.

KRETZ et al [8] have studied the effect of nickel

Corresponding author: C. S. RAMESH; Tel: +918026721983; Fax: +918026720886; E-mail: csr_gce@yahoo.co.in
DOI: 10.1016/S1003-6326(13)62428-0

coating on the SiC_p reinforced aluminium matrix composites. Nickel-coated SiC_p showed better bonding strength and hardness compared with uncoated SiC_p reinforced aluminium composites. ZHAN and ZHANG [9] have reported the mechanical and wear properties of uncoated and nickel-coated SiC_p/Cu composites. Nickel-coated SiC_p/Cu composites exhibited higher hardness, flexural strength, ductility and wear resistance compared with uncoated SiC_p/Cu composites. However, no information is available as regards the texture evolution in hot extruded aluminium based composites reinforced with nickel-coated SiC. The effect of nickel coating on SiCp on the development of texture during the hot extrusion is of particular interest from the fundamental point of view.

In the light of the above analysis, the present work aims at investigating the texture evolution in hot extruded SiC particles (uncoated and nickel coated) reinforced 6061 aluminium alloy composites.

2 Experimental

6061 aluminium alloy was reinforced with SiC particles having size in the range of 5−30 μm. SiC_p composites were coated with nickel by electroless plating method. The detailed procedure for electroless coating was described in Ref. [10]. The composite was fabricated by stir casting method with both the uncoated and nickel coated SiCp composites of 10% in mass fraction. The cast composite billets were hot extruded at 843 K adopting an extrusion ratio of 15.5:1. The samples were cut from mid sections of the extruded rods using a slow speed diamond cutter and electro-polished using an electrolyte of 20% perchloric acid + 80% methanol at −20 °C and 15 V (DC). The electropolished samples were subjected to texture analysis using the OIM system on a FEI Quanta 200 HV scanning electron microscope (SEM).

The crystallographic texture was determined from the orientation distribution functions (ODFs). ODFs were calculated using four incomplete pole figures (100), (110), (111) and (113). The ODFs are displayed using the Bunge's notation, which are represented in Euler's space at constant φ_2. The volume fractions of the texture components were also obtained from the ODFs using the MTM-FHM software [11].

3 Results and discussion

Figures 1(a), (b) and (c) show the SEM images of aluminium alloy (A1), uncoated (U1) and Ni−P coated SiC_p/Al 6061 (C1) composites respectively. SEM images clearly reveal uniformity in the distribution of SiC particles throughout the matrix. Figure 1(d) shows the strong interfacial bonding between the aluminium 6061 alloy matrix and Ni−P coated SiC particles. The

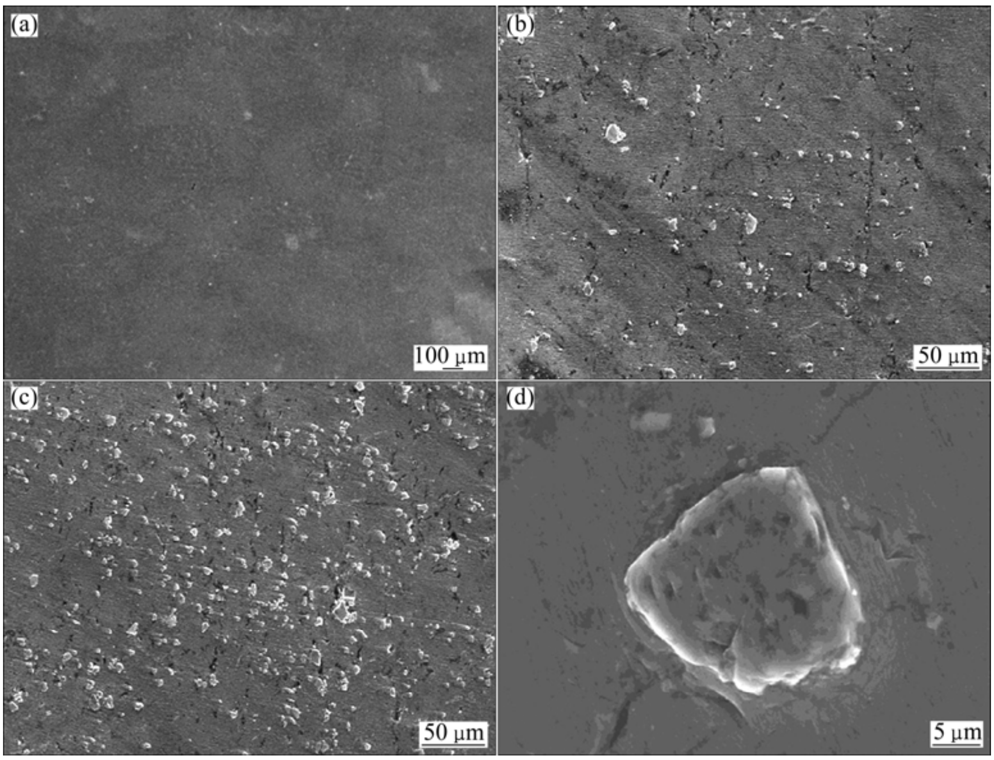

Fig. 1 SEM images of hot extruded Al alloy, uncoated and nickel-coated SiC_p/Al composites: (a) 6061 aluminium alloy; (b) Uncoated 10% SiC_p/Al 6061 composite; (c) Nickel-coated 10% SiC_p/Al 6061 composite; (d) Ni−P coated SiC_p particle exhibiting good bonding with Al 6061 matrix

uniform distribution and good bonding of SiC particles can be mainly attributed to enhanced wettability of Ni−P coated SiC particles in molten metal during the preparation of composites.

Figures 2(a), (b) and (c) show the EBSD images of partially recrystallized alloy A1, composite C1 and fully recrystallized composite U1. In both alloy A1 and composite C1, the elongated grains are perfectly oriented in the direction of extrusion resulting in the strong texture. In the case of composite U1, weak texture has been observed whose maximum intensity does not exceed 8× random. The weak texture of composite is due to the interaction of matrix with the SiC_p which disrupts the flow of matrix. These large and non-deformable SiC_p particles are associated with a zone of lattice rotation which disrupts the normal deformation texture.

Figure 3 shows the inverse pole figures of A1, C1 and U1. From the inverse pole figures, it is observed that ⟨101⟩ directions are parallel to extrusion direction in U1 and A1 while ⟨111⟩ directions are parallel to extrusion direction in C1. Figures 4(a−c) show the ODFs of alloy A1, composites C1 and U1. The ODFs of alloy A1 and composites C1 do exhibit the typical FCC texture, in which most of the orientations are assembled along the β fiber that runs through the Euler space from brass (110)⟨112⟩ through the S (123)⟨634⟩ to Cu (112)⟨111⟩. The textures of both A1 and C1 exhibit strong S and Cu orientations along with fairly mild cube texture. It is observed that S orientation possesses high dislocation density compared with the other orientations [12]. The intensity of S component in alloy A1 and composite C1 is high whereas in composite U1 the intensity is low. This implies that the cube orientation has grown at the expense of S in composite U1.

The evolution of texture in composite U1 displays the combination of cube orientation (001)⟨100⟩, rotated cubes (CG (021)⟨100⟩ and CH (001)⟨120⟩) and Goss (110)⟨001⟩. The texture displays the combination of both

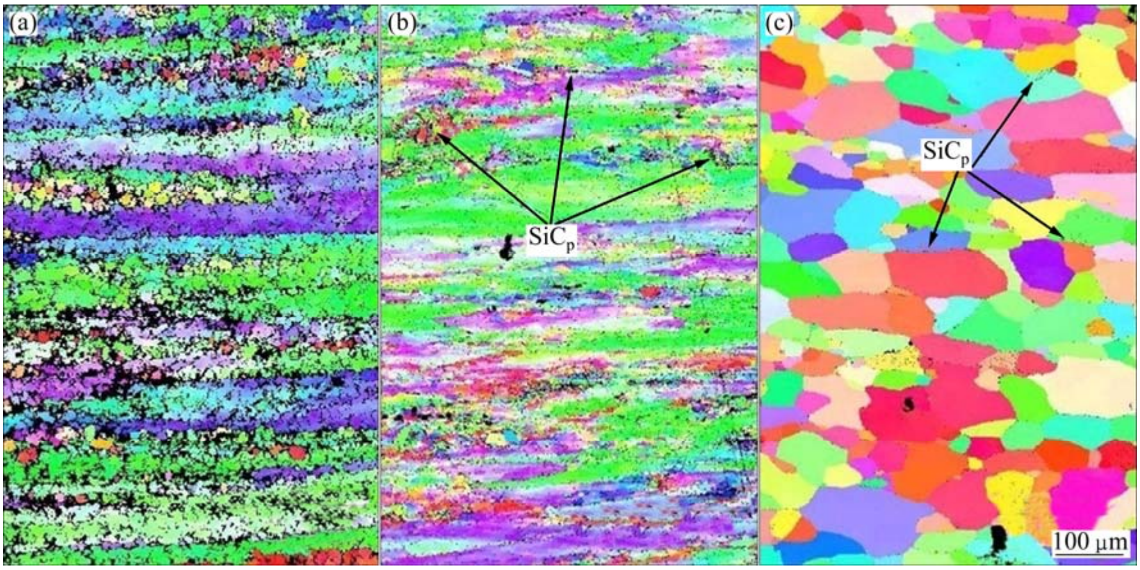

Fig. 2 Electron backscattered images of 6061 aluminium alloy (a), 10% nickel coated SiC/Al 6061 composite (b) and 10% uncoated SiC/Al 6061 composite (c) extruded at 843 K

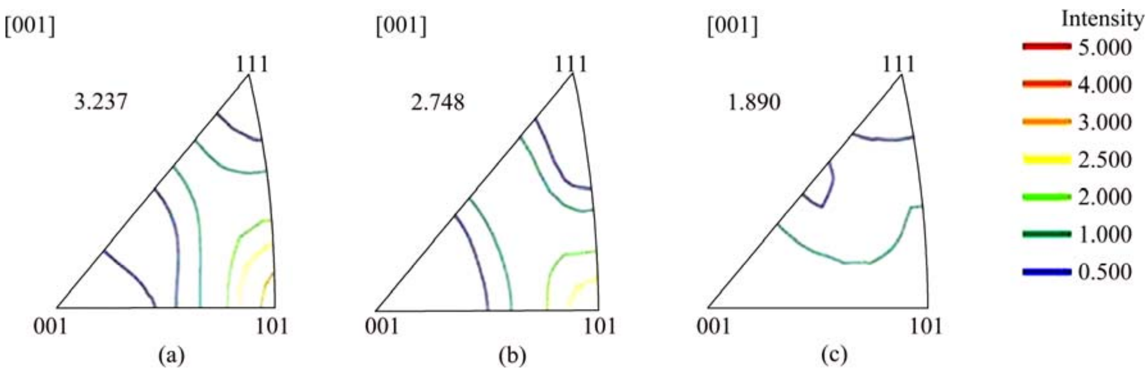

Fig. 3 Inverse pole figures of hot extruded 6061 aluminium alloy (a), 10% nickel-coated SiC_p/Al 6061 composite (b) and 10% uncoated SiC_p/Al 6061 composite (c)

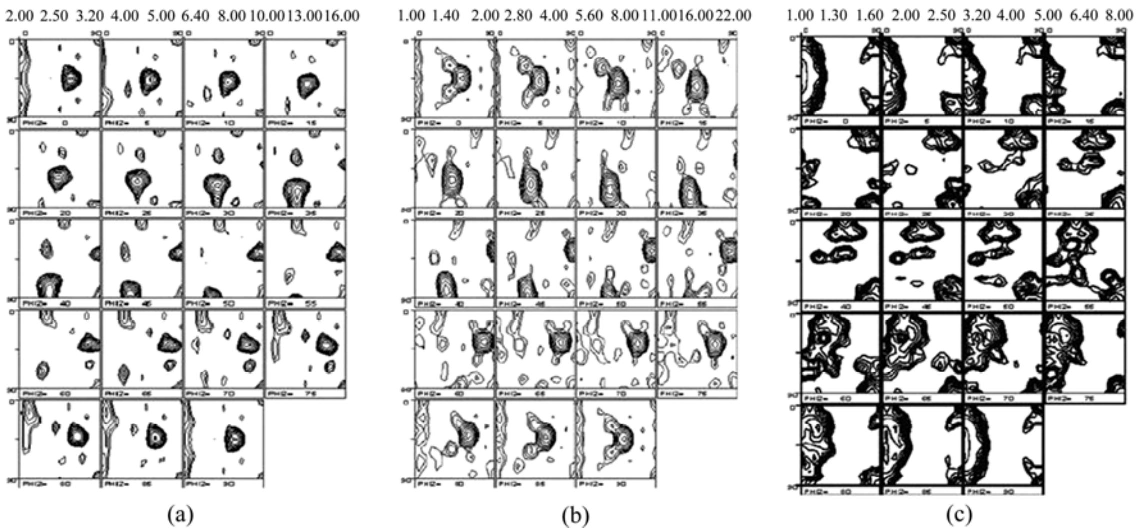

Fig. 4 Orientation distribution functions of hot extruded 6061 aluminium alloy (a), 10% nickel-coated SiC_p/Al 6061 composite (b) and 10% uncoated SiC_p/Al 6061 composite (c)

PSN and cube orientation. Though the formation of cube band in this case is hard to explain, a potent source of these grains is the original cube grains which were present in the undeformed state [13]. In order to analyze the recrystallization texture in composite C1, a brief review of recrystallization texture in aluminium and its alloys containing second phase particles is discussed below. When the composite is subjected to work hardening, the flow of matrix encounters the hard SiC particles leading to rotation of matrix subgrains in the vicinity of the particles generating dislocations. The dislocations thus produced around SiC particles leads to the formation of deformation zone [14]. These deformation zones are preferable sites for the nucleation of recrystallization termed as particle stimulated nucleation which depends on particle size, strain rate and working temperature [15,16]. On the other hand, at higher deformation temperatures the dislocations may be able to climb around the second phase particles preventing the formation of deformation zones. This can generate different types of textures which largely influence the recrystallization of hot deformed alloy or composite, particularly cube orientation in aluminium alloys.

At high deformation temperature, the effect of PSN is highly negligible. The PSN as a function of temperature is mainly dependent on the Zener−Hollomon (Z) factor. This factor relates both the strain rate and working temperature by expression (1):

$$Z = \dot{\varepsilon} \exp\left(\frac{Q}{RT}\right) \tag{1}$$

where $\dot{\varepsilon}$, Q and T are strain rate, activation energy and thermodynamic temperature respectively. At lower Z or higher working temperature, the stored energy associated with different orientations is expected to diminish. The stored energy concept may not work in the present composite U1 which is deformed at higher temperature. Further PSN is also expected to diminish at lower Z value [17]. Hence the necessary criteria for PSN to occur do largely depend on the critical size of second phase particles. The critical particle size d_f of the second phase particles is given by expression (2):

$$d_f = \left(\frac{K_1}{TZ}\right)^{1/2} \tag{2}$$

where K_1 (1712 $m^2 \cdot s^{-1} \cdot K$) is a constant and T is the deformation temperature. Solving the above equation by considering particle size, d_f=5 μm and T=843 K, we obtain Z=8.12× 10^{10} s^{-1}. This value of Z fits well with the condition for PSN which is governed by deformation zone formation. Thus SiC particles with a size of ~5 μm act as potential PSN sites.

In composite U1 the recrystallization texture can be explained by considering the rotated grains (CG (021)⟨100⟩ and CH (001)⟨120⟩), which is one of the means to distinguish the PSN and non-PSN regions. From Fig. 5, we can observe that the volume fraction of rotated cubes is more in composite U1. The contribution from the rotated cube and Goss in composite U1 is larger than that in alloy A1 or composite C1, which clearly indicates the recrystallization process. In addition, we can observe the randomized and weak recrystallization texture due to PSN. This phenomenon holds in a good agreement with more equiaxed grain structures in composite U1 in comparison to the unreinforced alloy A1. Hence, one can conclude that PSN is one of the possible mechanisms for the recrystallization in composite U1.

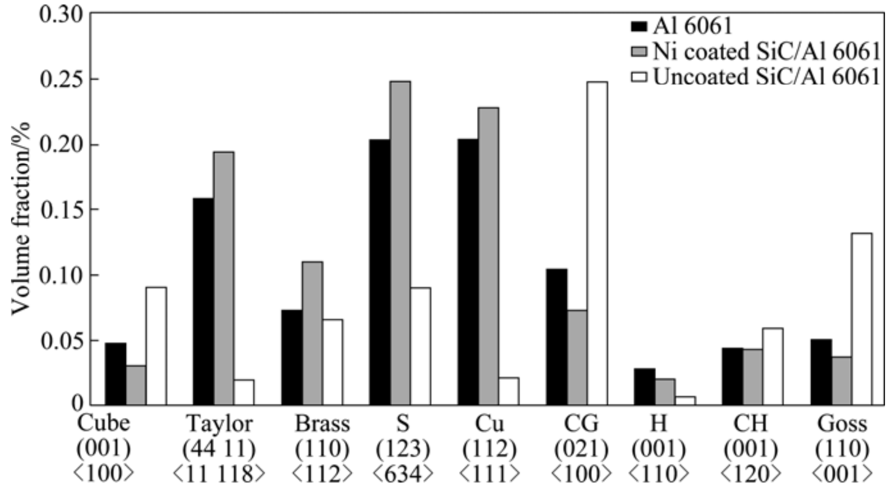

Fig. 5 ODF estimated volume fractions of different texture components of 6061 aluminium alloy, 10% nickel-coated and uncoated SiC_p/Al 6061 composites

4 Conclusions

The alloy and composite with uncoated SiC_p showed the presence of strong β fiber along the extrusion axis with a small amount of cube texture. The intensities of S and Cu are stronger along the β fiber. Hot extruded Al 6061 composite with uncoated SiC_p exhibited a stronger cube (001)⟨100⟩ and Goss component (110)⟨001⟩ indicating the recrystallization of the composite with equiaxed grains. At a deformation temperature of 843 K, PSN is the dominant mechanism for the recrystallization in Al 6061 composite with nickel-coated SiC_p, which is governed by the deformation zone formation rather than stored energy.

Acknowledgements

The authors acknowledge DST, New Delhi for granting financial assistance to carry out this work which is a part of research project No. SR/S3/ME/019/2004-SERC. The authors also acknowledge National Facility of Texture and OIM−supported by DST (IRPHA) IIT, Bombay for their support in carrying out the texture studies. The critical and useful discussions of the manuscript by Dr. N. ESHWARA PRASAD and Dr. A. K. SINGH, DMRL is also acknowledged.

References

[1] CHRISTMAN T, NEEDLEMAN A, SURESH S. An experimental and numerical study of deformation in metal-ceramic composites [J]. Acta Metallurgica, 1989, 37: 3029−3050.

[2] CHAWLA K K. Metal matrix composite [C]//CAHN R W, HANSEN P, KRAMER E J. Structure and Properties of Composites. New York: VCH publishers Inc. 1993.

[3] POUDENS A, BACROIX B. Recrystallization textures in Al−SiC metal matrix composites [J]. Scripta Materialia, 1996, 34: 847−855.

[4] ZHANG W L, GU, WANG D Z, YAO Z K. Rolling and annealing textures of a SiC_w/Al composite [J]. Materials Letters, 2004, 58: 3414−3418.

[5] POUDENS A, BACROIX B, BRETHEAU T. Influence of microstructures and particle concentrations on the development of extrusion temperatures in metal matrix composites [J]. Materials Science and Engineering A, 1995, 196: 219−228.

[6] BORREGO A, FERNANDEZ R, CRISTINA M C, IBANEZ J, DONCEL G G. Influence of extrusion temperature on the microstructure and the texture of 6061Al−15vol.% SiC_w PM composites [J]. Composites Science and Technology, 2002, 62: 731−742.

[7] HUMPHREYS F J. The thermomechanical processing of A1−SiC particulate composites [J]. Materials Science and Engineering A, 1991, 135: 267−273.

[8] KRETZ F, GACSI Z, KOVACS J, PIECZONKA T. The electroless deposition of nickel on SiC particles for aluminum matrix composites [J]. Surface and Coatings Technology, 2004, 180−181: 575−579.

[9] ZHAN Y, ZHANG G. The effect of interfacial modifying on the mechanical and wear properties of SiC_p/Cu composites [J]. Materials Letters, 2003, 57: 4583−4591.

[10] RAMESH C S, KESHAVAMURTHY R, CHANNABASAPPA B H, PRAMOD S. Friction and wear behaviour of Ni−P coated Si_3N_4 reinforced Al6061 composites [J]. Tribology International, 2010, 43: 623−634.

[11] VAN-HOUTTE P. MTM-FHM software system, version 2 [R]. Belgium: MTM, KULeuven, 1995.

[12] SAMAJDAR I, DOHERTY R D. Cube recrystallization texture in warm deformed aluminum: understanding and prediction [J]. Acta Materialia, 1998, 46: 3145−3158.

[13] GUIGLIONDA G, BORBELY A, DRIVER J H. Orientation-dependent stored energies in hot deformed Al−2.5%Mg and their influence on recrystallization [J]. Acta Materialia, 2004, 52: 3413−3423.

[14] ASHBY M F. The deformation of plastically non-homogeneous

materials [J]. Philosophical Magazine, 1970, 21: 399−424.
[15] HUMPHREYS F J, HATHERLY M. Recrystallization and related annealing phenomena [M]. 2nd ed. Elsevier, 2004.
[16] DU Yu-xuan, ZHANG Xin-ming, YE Ling-ying, LIU Sheng-dan. Evolution of grain structure in AA2195 Al−Li alloy plate during recrystallization [J]. Transactions of Nonferrous Metals Society of China, 2006, 16: 321−326.
[17] HUMPHREYS F J, KALU P N. Dislocation-particle interactions during high temperature deformation of two-phase aluminium alloys [J]. Acta Metallurgica, 1987, 35: 2815−2829.

颗粒激发形核在热挤压 Al6061/SiC$_p$ 复合材料再结晶过程中的作用

C. S. RAMESH[1,2], R. KESHAVAMURTHY[3], Praveennath G. KOPPAD[1], K. T. KASHYAP[1]

1. Department of Mechanical Engineering, PES Institute of Technology, Bangalore 560085, India;
2. Visiting Professor, School of Design, Engineering and Computing, Bournemouth University, United Kingdom;
3. Central Manufacturing Technology Institute, Tumkur Road, Bangalore 560022, India

摘 要：采用电子背散射衍射技术，研究 SiC$_p$ 增强热挤压 Al6061 铝合金复合材料的织构和微观组织演变。Al6061 铝合金及其 Ni 包覆 SiC$_p$ 增强的复合材料织构中都存在强的 β 纤维，其轴平行于挤压方向。在未用 SiC$_p$ 增强的热挤压 Al6061 铝合金中，除了主要的立方织构 001)⟨100⟩，在完全再结晶晶粒中也存在部分等轴结构。这种再结晶织构的出现归因于粒径小于 5 μm 的 SiC$_p$ 粒子的形成而产生的粒子激发形核。在这些条件下，低 Z (~ 10^{12} s^{-1})值证实了粒子激发形核是再结晶的主导机制之一，且受变形区的形成而非储能的控制。

关键词：金属基复合材料；6061/SiC$_p$ 复合材料；挤压；粒子激发形核；再结晶；储能

(Edited by Hua YANG)